

Synthesis Of NiO Doped ZnO/MWCNT Nanocomposite And Its Charecterization For Photocatalytic & Antimicrobial Applications

D. Saravanakkumar^{1,*}, R. Karthika², S. Ganasaravanan³, S. Sivaranjani⁴,
S.Pandiarajan², B. Ravikumar², A. Ayeshamariam^{3*}

^{1,*} Research and Development Centre, Bharathiyar University, Coimbatore, 641046, Tamilnadu, India

²Department of Physics, Devanga Arts College (Autonomous), Aruppukottai, 626101, Tamilnadu, India

^{1,3,*}Department of Physics, Khadir Mohideen College, Adirampattinam – 614 701, Tamilnadu, India

⁴Department of Physics, SBM College of Engineering and Technology, Dindigul- 624 005, Tamilnadu, India

*Corresponding Authors: D. Saravanakkumar, A. Ayeshamariam

Abstract: The field of Bionanoscience is one of the vibrant research area in smart materials, antimicrobial activity and drug delivery system. Cost effective method of simple pyrolysis treated synthesis of nanoparticles is the present research in branch of nanobioscience. The NiO doped nanocomposite synthesized simply have been widely used in the anti microbial techniques and waste water management. In this research article we present a simple and cost effective method synthesis of NiO doped ZnO/MWCNT nanocomposite. This composite were structurally and morphologicaly charecterized by Powder X-Ray Diffraction (PXRD) and Field Emission Scanning Electron Microscope (FESEM). It was optically chrecterized by the Ultra-Violet Visible (UV-Vis) spectroscopy and Fourier Transform Infra-Red (FTIR) spectroscopy. Further these charecterized by Energy Dispersive X-Ray spectroscopy for percentage of elemental compositions. Moreover these synthesized nanocomposite was found to be very effective antibacterial agents against *Staphylococcus aureus* and *pseudomonas aeruginosa* and also effective antifungal candidates for *Aspergillus niger* and *Candida albicans* for various quantities in μL . Finally it was to be a good photocatalytic behavior material for photodegradation when interact with *Methyl Orange (MO)* dye by separating electron hole pair effectively.

Keywords: Nanocomposites, XRD, FESEM, Antibacterial, antifungal and Photocatalytic.

Date of Submission: 29-05-2018

Date of acceptance: 14-06-2018

I. Introduction

ZnO nanoparticles (NPs) have high photosensitivity, photocatalytic activity, quantum efficiency, non-toxicity and low cost. Its extraordinary structural benefits further extends their applications to chemical sensors, transparent conductor, gas sensors, varistors, solar cells, light-emitting diodes, surface acoustic wave filters, photonic crystals, photodetectors, photodiodes and optical modulator waveguides. These applications are due to their wide bandgap (3.37 eV), energy (60 meV), excellent chemical stability and thermal stability [1-6].

Among various p-type oxides, nickel oxide (NiO) is a highly active material with wide band gap (3.6 eV to 4.0 eV) and extensively studied for various applications such as catalysis, gas sensing, battery cathodes, magnetic materials, electrochromic films, chemical sensors and photovoltaic devices. MWCNTs have a highly porous and hollow structure, large specific surface area, significant electronic and conductive properties and a versatile surface that can be modified to improve adsorption properties. The fabrications of ZnO/multi-walled carbon nanotube (MWCNT) nanocomposites have gained interest among the materials because of its superior optoelectronic properties, photocatalytic properties and their antibacterial activities. Since there has been an increase in the number of diseases due to bacterial transmission either by interpersonal or through contaminated surfaces ZnO, NiO and CNT particles are a less toxic and inhibition properties against harmful bacteria which causes disease in human body. Microorganisms such as *Escherichia coli* and *Staphylococcus epidermis* are bacterial pathogens in hospital environments that could be acquired even from an inanimate object [7-10]. Many synthesis techniques are available in preparation of metal oxide and MWCNT nanocomposite powder. Among them, some methods are combustion method, sol-gel method, sol-gel combustion method, coprecipitation method, modified sol-gel method, conventional spray pyrolysis method and soft chemical root method. Simplified Spray Pyrolysis (SSP) method is one of the cost effective method for synthesising a metaloxide nanopowder with excellent polycrystallinity nature [11-14].

In the present work, NiO doped ZnO/MWCNT (NiO:ZnO/MWCNT) nanocomposite powder were synthesised by SSP method and their structural, optical and antibacterial effects were investigated [15-19]. The sample were characterised by powder X-ray diffraction (XRD), Fourier Transform Infrared spectroscopy (FTIR),

Ultraviolet-Visible (UV-Vis) spectroscopy. The final compound is considered as good catalytic member in the UV-Visible photon shower in employing photo catalytic study to find out the degradation of MO dye. The antibacterial activity of the NiO:ZnO/MWCNT nanocomposite due to its inhibition on gram positive and gram negative bacteria under well diffusion process was studied. Similarly antifungal activity was also carried out to inhibit the harmful fungal organism.

II. Experimental procedure

In the synthesis of NiO:ZnO/CNT nanocomposite, the aqueous solution (0.2 M) of zinc acetate dissolved in 40ml of distilled water and stirred for 10 minutes. Then (0.2 M) of Nickel acetate and 0.1 mg of MWCNT are added to the above solution and mixture was continuously stirred for 30 minutes. A solution (0.1 M) of NaOH was added drop wise into the above solution under vigorous stirring for 12 hours. The stirred solution was transferred into well cleaned perfume spray bottle. The solution was sprayed periodically (10 s interval for each spray) on the surface of hot copper plate. The resulting product was collected from the copper plate and replaced to quartz crucible in muffle furnace at 550°C. This calcined resultant powder was crushed in Fresco Granite Mortar And Pestle - Black for 2 Hrs to get fine NiO:ZnO/CNT nanocomposite powder.

III. Characterization

Crystallographic structural data characterization of the synthesized sample was carried out by X-ray diffraction using an X'Pert Pro with minimum step size Omega: 0.001° and CuK α radiation, $\lambda = 1.5406 \text{ \AA}$. Field emission scanning electron microscopy images were recorded on an FEI-Quanta-FEG 250 operating at 30 kV and equipped with an energy dispersive X-ray spectroscopy (EDX) detector. Vibrational functional groups in the sample were studied using the Fourier transform infrared spectrum of the Bruker Tensor 27 at TR mode in the wave number range 400–4000 cm^{-1} . The absorption spectrum was recorded using a JOSCO UV-Vis spectrophotometer in the wavelength range 190–900 nm. The well diffusion method was employed for antibacterial and antifungal studies.

IV. XRD Analysis

Diffraction peaks for the NiO:ZnO/CNT nanocomposite become sharper and the full width at half maximum of the peaks is narrower than others, indicating the excellent crystal quality resulting from water medium as solvent and hot copper plate act as very good evaporator of impurities.

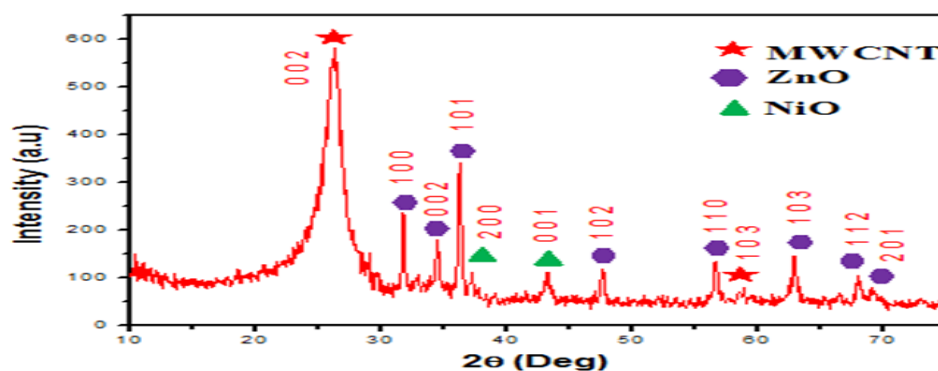


Figure 1: The XRD pattern of NiO:ZnO/MWCNT nanocomposite calcinated at 550°C. The XRD pattern shows that the sample product is polycrystalline with different multi phase

Structural parameters like Crystallite size were calculated using Debye - Scherrer formula $D = \frac{0.9\lambda}{\beta \cos\theta}$ (nm), Where D is the crystallite size, λ is the wavelength of the X-ray employed Cu K α radiation (0.154nm), β is the Full Width at Half Maximum (FWHM) of the peaks, θ is the Bragg angle obtained from 2θ value. Dislocation Density δ is a measure of amount of defects and vacancies in the crystal which can be determined from the crystallite size (D) using the formula, $\delta = \frac{1}{D^2}$ lines/m².

In order to understand the structure of the NiO:ZnO/MWCNT composite, PXRD has been recorded. Figure 1 shows the XRD pattern of the NiO doped with ZnO/MWCNT nanoparticles. Powder X-ray diffraction measurements were performed using Philips XRD Powder diffractometer (PW3050/60) with Cu K α radiation ($\lambda = 0.15406 \text{ nm}$). The peaks at 2θ values of 31.73° , 34.40° , 36.22° , 47.57° , 56.52° , 62.84° , 67.91° and 69.11° corresponded to the crystal planes of (100), (002), (101), (102), (110), (103), (112) and (201) of ZnO nanoparticles [20-23]. The XRD peaks reveal good agreements with ZnO (JCPDS No. 36-1451). Moreover, the

peaks at 2θ values of 37.12° and 43.15° correspond to the crystalline planes (200) and (001) respectively. These peaks reveal a good agreement with NiO (JCPDS. 89-7131) [24-26]. In addition, the prominent peak about $2\theta = 26.214^\circ$ can be attributed to the (0 0 2) reflection of MWCNT (JCPDS. 75-1621). The average crystallites size was calculated by the Scherrer's formula and found to be in the range of 39 nm [27-30]. Table 1 shows some geometric parameters of nanocomposite such as observed 2θ values, full width at half maximum values of peak, crystallite size and lattice strain. Dislocation density is a measure of the distribution of lattice strain arising from crystal imperfections, such as lattice dislocations.

Compounds	JCPDS Card No.	2 θ Values (Deg)		FWHM β		Grain Size (nm)	Dislocation density Lines/m ² 10 ¹⁵
		Standard	Observed	Deg	(rad) 10 ⁻³		
Zno	36-1451	36.253	36.245	0.1968	3.4243	42.58	0.5515
Carbon(MWCNT)	75-1621	26.228	26.214	0.8856	15.4094	09.23	11.738
NiO	89-7131	37.250	37.123	0.2952	5.1364	28.46	01.234

Table 1: Structural Data: Angle of diffraction 2 θ , value of Full Width at half Maximum (FWHM), and dislocation density of NiO:ZnO/MWCNTnanocomposite calculated from XRD data.

V. Fesem Analysis

Field Emission Scanning Electron Microscope with high resolution is powerful instrument for imaging of fine structures of NiO:ZnO/CNT nanocomposite synthesized by SSP Method for morphology investigation.

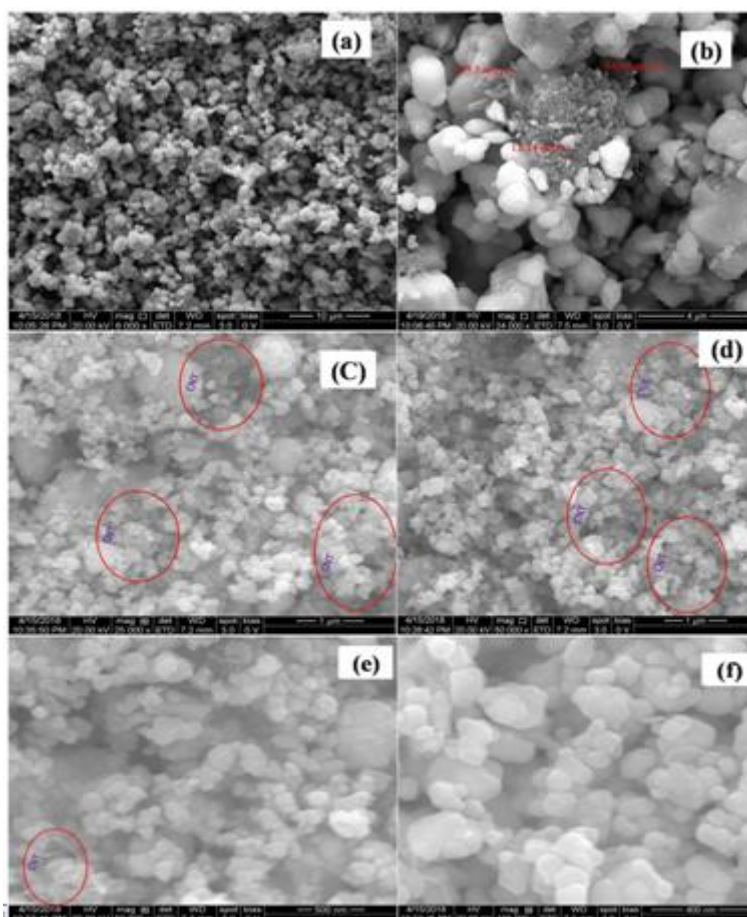


Figure.2: (a-f) FESEM images of NiO: ZnO/CNT nanocomposite synthesized by SSP method

Figures 2 (a-f) shows the FESEM images of the NiO:ZnO/CNT nanocomposite. Figure 2 (b) shows the noodle like, thin curved worms like and curling hair like morphology of MWCNT of the composite. In the Figures 2 (c-f), spheroid-like and plate like morphology of nanoparticles with the MWCNTs are appeared. From this observation it is revealed that these spheroids like particles were considered to be ZnO nanoparticles and plate

like particles were considered to be NiO nanoparticles. Therefore, this cost effective SSP method resulted in successful synthesis of NiO:ZnO/MWCNT nanocomposite. Moreover, it can be seen that in the fig. 2 (d-f) with increasing the molar concentration ratio of MWCNT precursor to ZnO, the number MWCNT on the surface of the granular rough surface are increased. It was observed that MWCNTs were covered with ZnO and NiO nanoparticles. ZnO and NiO nanoparticles were ununiformly dispersed with MWCNT surface and in some where zones, bundles of MWCNT were found with irregular agglomerate dispersion. The MWCNTs with high specific surface area can act as a reactive zone for a nucleation of the NiO and ZnO. Therefore, their smaller sizes may be applicable for redox action of the both ZnO and NiO with higher specific surface area [31].

VI. EDAX Analysis

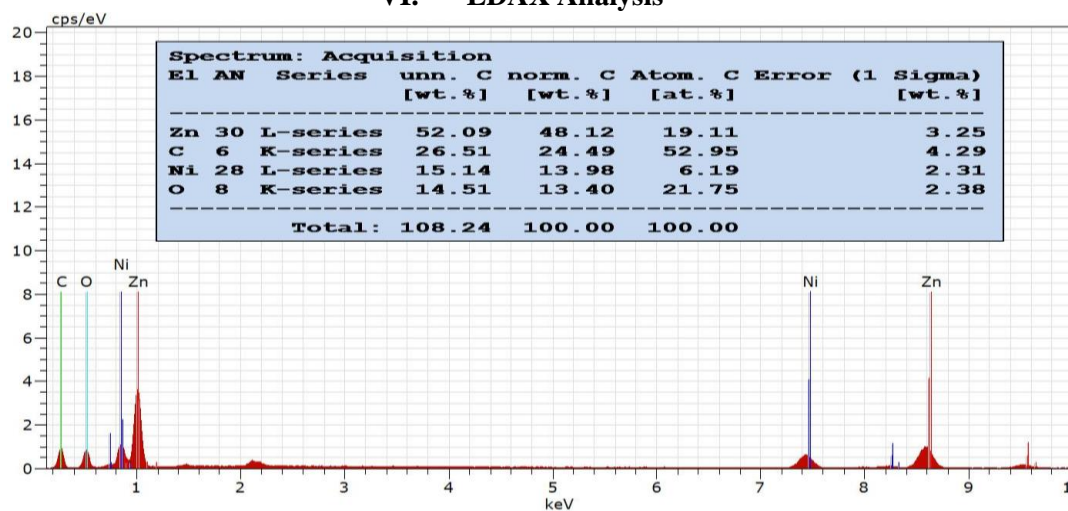


Figure 3: EDX spectrum of NiO:ZnO/MWCNT nanocomposite synthesized by the SSP method where the inset represents the percentage of elementals composition.

Figure 3 shows the EDX spectrum of NiO:ZnO/CNT nanocomposite. Energy dispersive X-ray spectroscopy (EDX) is used for further confirmation leading to presence of functionalized NiO, ZnO, MWCNT composite. Thereby, we can emphasize the presence of C, Ni, O and Zn elements in the composite sample. The acquisition in EDAX spectrum for quantitative elemental analysis results of NiO:ZnO/CNT was performed in the specific zone shown in Figure 3 and revealed that the only the wt% of oxygen (O), Nickel (Ni), carbon (C), Zinc (Zn) on the surfaces were 13.40, 13.98, 24.49 and 48.12 % of signals were detected respectively. The elemental mapping also demonstrated that the MWCNTs and NiO are densely decorated with ZnO NPs. The average composition of NiO:ZnO/MWCNT contains a Zn:C:Ni:O atomic ratio of 19:53:6:22 which was represented in the inset of Figure 5.3. This experimental observation is very close to expected NiO composition of 14 wt%. So no other signal of secondary phase was detected as shown in Figure 5.3. This indicates the better purity of chemical composition used in this study.

VII. FT-IR Analysis

In the present study the FTIR is utilized in order to analyze the possible bonding between the neighboring structures and the surface of the MWCNTs. In other words, FTIR in this study could be a means in exhibiting the interactions at the surface during the possible adsorption of nanoparticles and to determine the structure of the adsorbed species. Figure 4 presents the FTIR spectrum of NiO:ZnO/CNT nanocomposite recorded in the range of 4000 - 400 cm^{-1} . The spectrum shows a broad band at 3322 cm^{-1} , which refers to the -OH stretching of the hydroxyl group that can be ascribed to the oscillation of water molecule, bound on the surface of the sample.

The band at 1579 cm^{-1} corresponds to the stretching vibration of $\text{C}\equiv\text{C}$ bond and it is associated with the vibration of the carbon skeleton of the MWCNT. The band at 1369 cm^{-1} is assigned as the rocking mode of vibration of C-H bonds. The band located near 1100 cm^{-1} can be attributed to the Ni-O-Ni stretching mode. The observed peak at 601 cm^{-1} (weak - broad) and 433 cm^{-1} denote the formation of metal-oxide (Ni=O) and Zn-O bond which recognized the configuration of the NiO:ZnO/MWCNT groups [32-36]. The result obtained from FTIR spectrum suggested that the existed hydroxyl group and $\text{C}\equiv\text{C}$ group associated with NiO and MWCNTs which have been covered by almost of surface active sites of ZnO NPs responsible for antimicrobial activities.

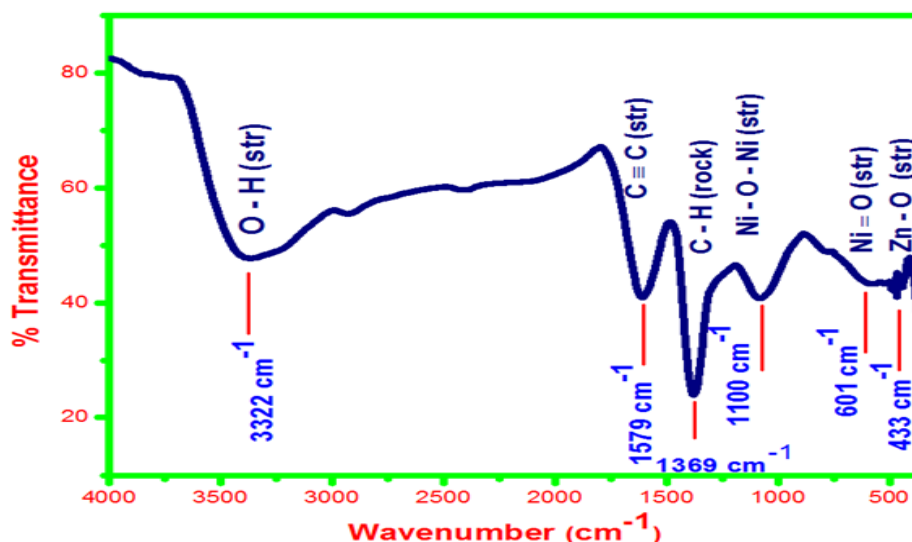


Figure 4: FT-IR spectrum of NiO:ZnO/MWCNT nanocomposite

VIII. UV-Vis Analysis

The UV/Vis spectra of the NiO:ZnO/MWCNT nanocomposite were recorded in the visible range (400–800 nm) and an absorption band at around ~200.0 nm was found (Figure 5). Figure 6 shows the optical transmittance spectrum of NiO:ZnO/MWCNT nanocomposite in the wavelength range from 200 to 800 nm. The transmittance is calculated from measured absorbance (α) at a certain wavelength of light (λ) using the formula: $A_{\lambda} = -\log_{10} T_{\lambda}$.

The composites are not transparent in the visible range of the electromagnetic spectrum [37]. On the basis of the maximum level band absorption, the band-gap energies of the NiO:ZnO/CNT nanocomposite was calculated using Tauc's equation (v). $(\alpha h\nu)^{1/r} = A(h\nu - E_{bg})$, Where α is the absorption coefficient, A is the constant related to the effective mass of the electrons, $r = 0.5$ (Direct transition), h = Plank's constant, ν = Frequency and E_{bg} = Band-gap energy.

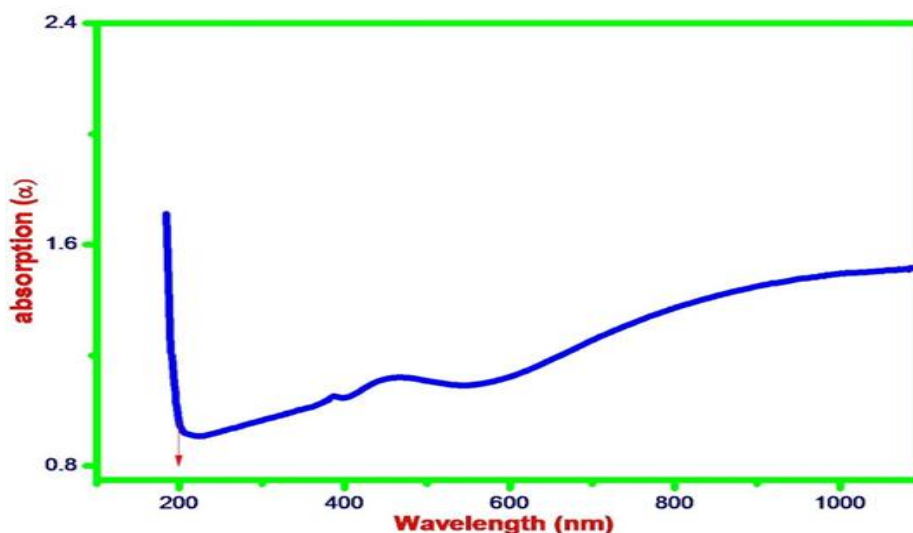


Figure 5: UV/Vis absorption spectra of NiO: ZnO/MWCNT nanocomposite. UV/Vis: ultra-violet visible

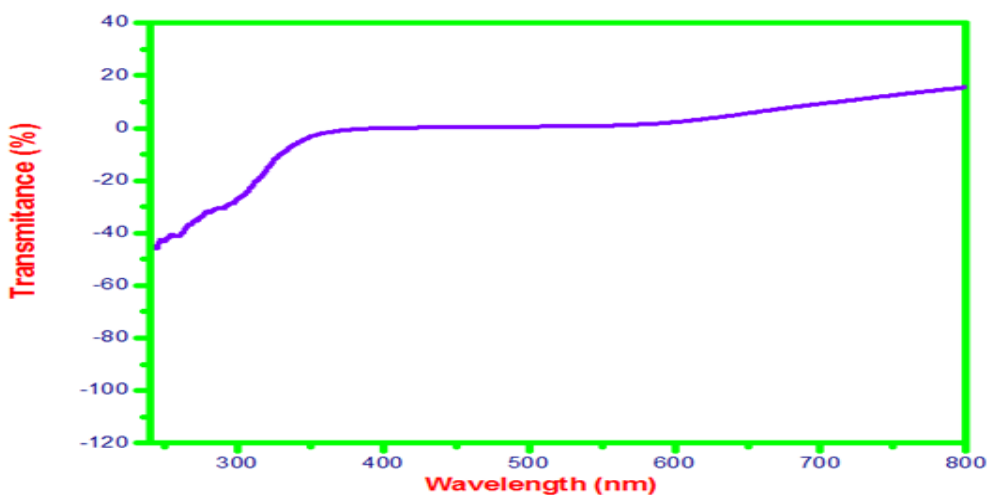


Figure 6: UV/Vis transmission spectra of NiO:ZnO/MWCNT nanocomposite

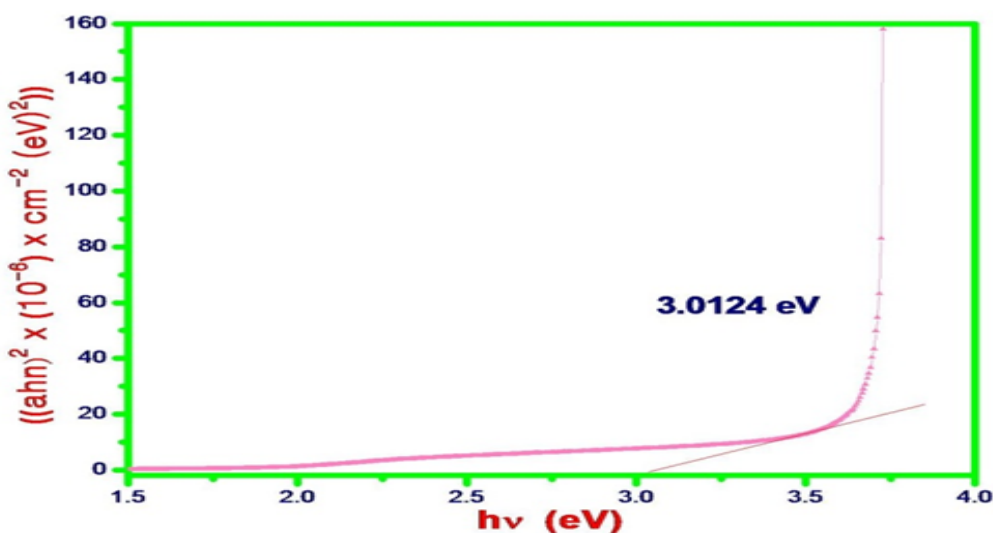


Figure 7: UV/Vis band-gap energy of NiO :ZnO/MWCNT nanocomposite.

According to the direct band-gap rule, $(\alpha h\nu)^2 = A(h\nu - E_{pg})$, curve of $(\alpha h\nu)^2 vsh\nu$ were plotted and then extrapolated to the axis. From the extrapolated curve, the band-gap energy for NiO:ZnO/CNT nanocompositewas calculated as 3.0124 eV (Figure 7). No additional peaks associated with impurities and structural defects were observed in the spectrum that indicated the crystalline characteristics of the prepared NiO:ZnO/CNT nanocomposite.

IX. Antibacterial study

In this present case, the antibacterial activity of prepared NiO:ZnO/CNT nanocomposite was deliberated against gram positive and gram negative bacteria namely a) staphylococcus aureus and b) pseudomonas aeruginosa. The antibacterial effect of the nanocomposite on microorganisms may be held through the electrostatic attraction of positive charged silver and negative charged cell surface of bacterial membrane [38]. Figure 8 (a and b) shows the zone of inhibition of bacteria such as staphylococcus aureus and pseudomonas aeruginosa by employing NiO:ZnO/CNT nanocomposite. Table 2 shows the diameter of inhibition zone in mm for the respective bacteria. The antibacterial activities were tested for various quantities of NiO:ZnO/CNT nanocomposite (5 μ l, 10 μ l, 15 μ l). Since the composite having smaller crystallite size and different crystalline phase with unique properties, expected zone of inhibition was observed. Depending on the surface area available for interaction, NiO:ZnO/CNT nanocomposite can bind with bacteria and disturb its permeability and respiration function.

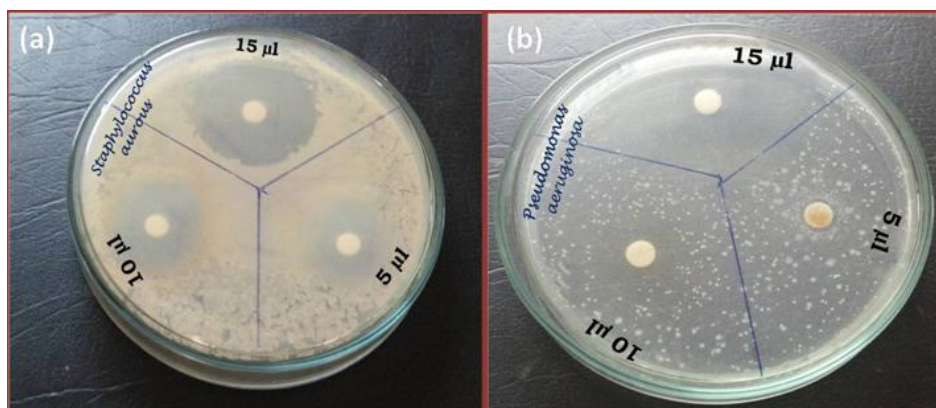
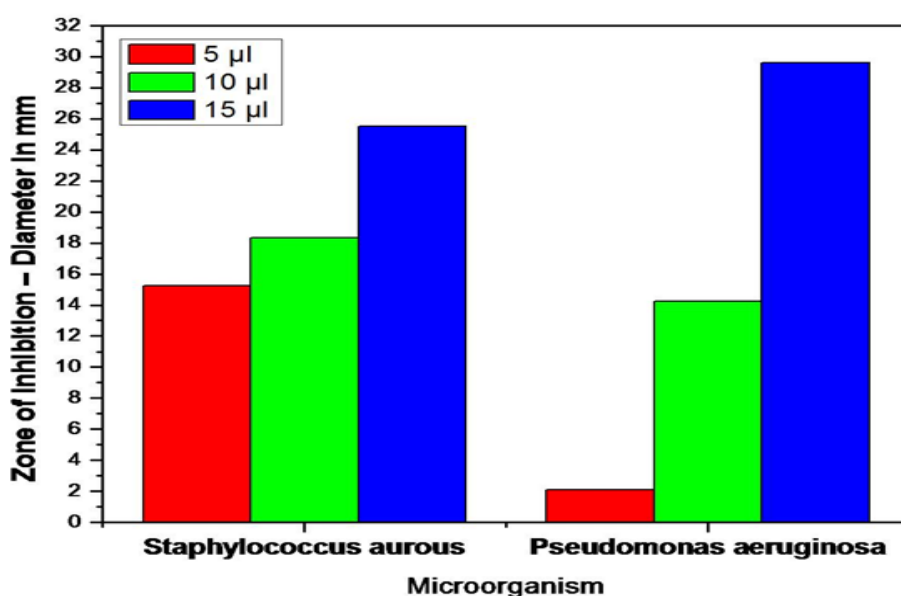


Figure 8: The photographic image of inhibition zones produced by NiO :ZnO/MWCNT nanocomposite against the bacteria a) Staphylococcus aureus and b) pseudomonas aeruginosa



Graph 1: Inhibition graph against Bacterial Strains a) Staphylococcus aureus and b) pseudomonas aeruginosa by NiO :ZnO/MWCNT nanocomposite

Table 2: Zone of inhibition in mm produced by NiO :ZnO/MWCNT nanocomposite against the bacteria a) staphylococcus aureus and b) pseudomonas aeruginosa

Microorganism	Zone of Inhibition – Diameter in mm		
	5µl	10µl	15µl
Staphylococcus aureus	15.26	18.32	25.51
Pseudomonas aeruginosa	2.12	14.25	29.63

Smaller grains having larger surface area can increase the ability to penetrate cell membrane and give more bactericidal effect than the larger particles [39, 40]. Thus, the antibacterial activity of prepared NiO :ZnO/MWCNT nanocomposite are influenced by the grain size and the effect of antibacterial activity increases with increasing the quantity from 5 µl to 15 µl nanocomposite (Graph 1) [49-50].

X. Antifungal Activity:

The antifungal effect of the nanocomposite on Aspergillus nigar and Candida albicans may be held through the electrostatic interaction of cell membrane or nucleus and nanocomposite [41, 42].

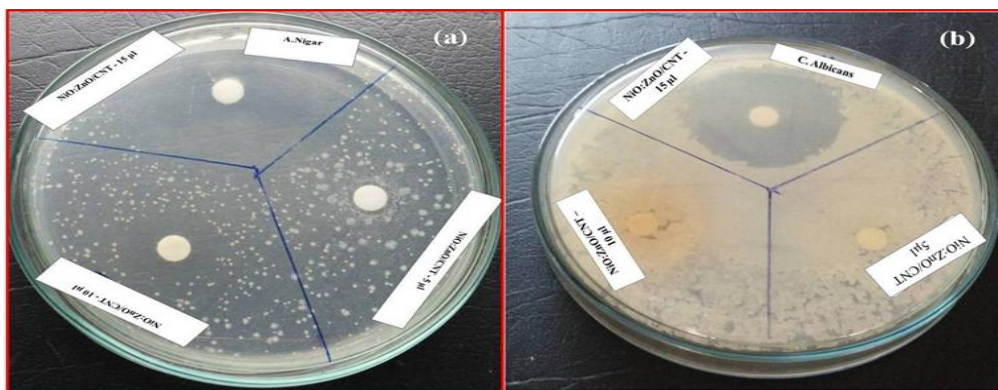
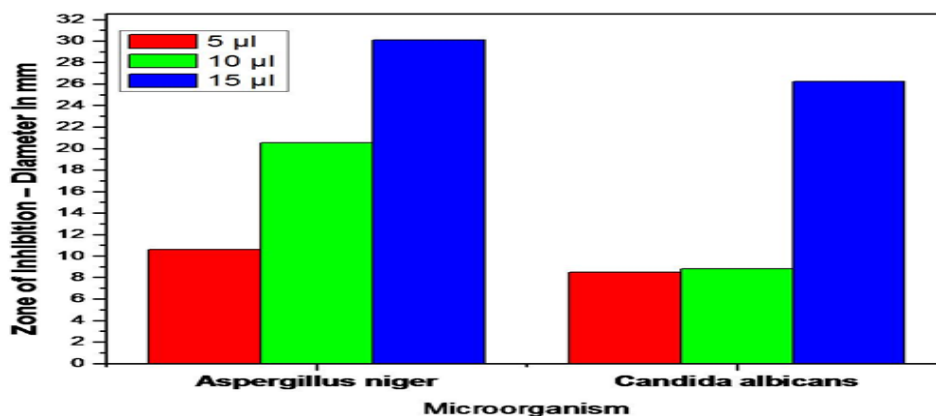


Figure 9: The photographic image of an inhibition zone produced by NiO :ZnO/MWCNT nanocomposite against fungi a) *Aspergillus niger* and b) *Candida albicans*.

Figure 9 (a and b) shows the zone of inhibition of NiO:ZnO/CNT nanocomposite against *Aspergillus niger* and *Candida albicans*. The antifungal activities were tested for various quantities of NiO:ZnO/CNT nanocomposite (5 µl, 10 µl, 15 µl). Table 3 shows the diameter of inhibition zone in mm for various quantity of prepared nanocomposite (Graph 2). The antibacterial activity of NiO:ZnO/CNT nanocomposite is effective because of its smaller crystallite size and different crystalline phase. Depending on the surface area available for interaction, NiO:ZnO/CNT nanocomposite can bind bacteria and disturb its permeability and respiration function.

Table 5.3: Zone of inhibition in mm produced by NiO :ZnO/MWCNT nanocomposite against the fungi a) *Aspergillus niger* and b) *Candida albicans*.

Microorganism	Zone of Inhibition – Diameter in mm		
	5µl	10µl	15µl
<i>Aspergillus niger</i>	10.6	20.5	30.1
<i>Candida albicans</i>	8.5	8.8	26.2



Graph 5.1: Inhibition graph plot against fungal pathogens a) *Aspergillus niger* and b) *Candida albicans* by NiO:ZnO/CNT nanocomposite

XI. Photo catalytic study:

In a photo reactor, internal light source of UV-Visible photon emitter which was surrounded by quartz jacket with specially designed cylindrical quartz cell was employed where MO dye solution was taken surrounded the light source. An external water jacket was used to maintain the constant temperature for over all reaction taking place by passing the cold water through it. Photocatalytic experiments were carried out by adding 0.05 g NiO:ZnO/CNT nanocomposites into photoreactor containing 20 ml of MO dye solution with an initial concentration of 5 mg/L.

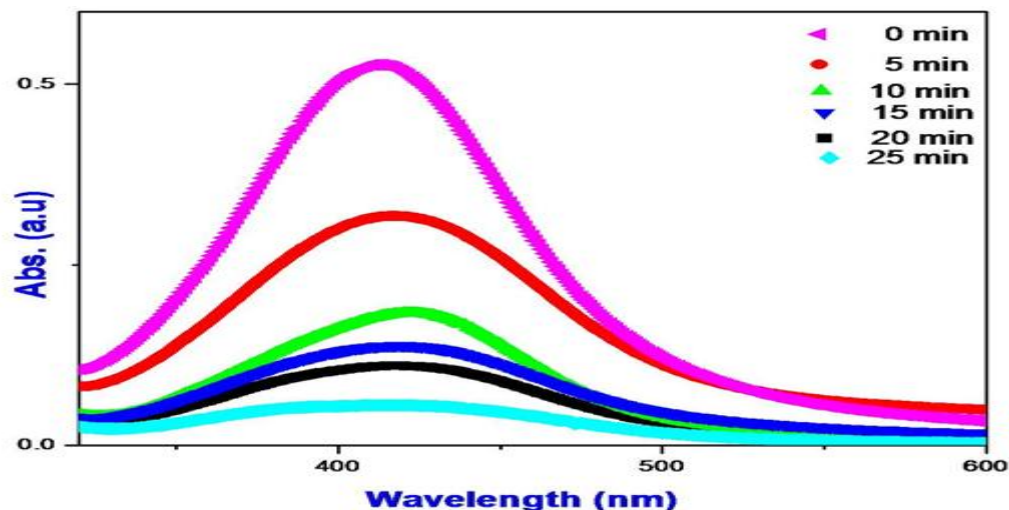


Figure 10: UV absorption spectral change of MO solution as a function of irradiation time NiO:ZnO/MWCNT nanocomposite. Concentration of MO= 5 mg/L, composite catalyst dose=0.05g/20ml.

The MO dye solution with catalyst was stirred in the darkroom for 10 h to reach the equilibrium of surface adsorption. Then the stirred suspensions were illuminated by UV-Visible Lamp (mercury lamp, 250 watt). The obtained solution was stirred continuously during the photocatalytic reaction up to 25 minutes as shown in the Figure 10. The change in color of MO concentration with the illumination time was increased and monitored by determining the absorbance at 430 nm using JOSCO UV-Vis spectrophotometer. At the reaction time of 25 minutes, the absorption peak decreased gradually. The mechanism of degradation follows a cascade of electron transfer from ZnO to MWCNT to NiO in the nanocomposite [43-46]. From this study, NiO:ZnO/MWCNT nanocomposite act as a good photocatalyst for MO dye degradation.

XII. Conclusion

NiO doped ZnO/MWCNT nanocomposite was successfully synthesized through cost effective SSP method with average crystallite size of 39 nm has been synthesized. Crystalline nature of the nanocomposite was evident from strong intensity peaks in the PXRD pattern. From the UV-Vis absorption spectrum, strong absorption at UV region of 200 nm and the band gap of NiO:ZnO/CNT nanocomposite were found to be 3.0124 eV. The FT-IR study confirmed the existence of $-C \equiv C$, Zn-O, Ni-O functional groups of NiO:ZnO/CNT nanocomposite. The prepared nanocomposite reveal good antimicrobial activity against gram positive and gram negative bacteria staphylococcus aureus, pseudomonas aeruginosa bacteria and good antifungal activity against both Aspergillus niger and candida albicans fungi. So the prepared nanoparticles have found applications in biomedical and water purification processes for inhibiting the growth of bacteria. Among all the nanocomposite materials, the ternary nanocomposite NiO:ZnO/MWCNT (Zn:C:Ni:O = 19:53:6:28) nanocomposite exhibits highest photocatalytic activity for degradation of Methyl Orange (MO) Dye using UV-Vis spectrophotometer irradiation.

References

- [1]. D.H.Piva, R.H.Piva, M.C.Rocha, J.A.Dias, O.R.K.Montedo, I.Malavazi, M.R.Morelli, Antibacterial and photocatalytic activity of ZnO nanoparticles from $Zn(OH)_2$ dehydrated by azeotropic distillation, freeze drying, and ethanol washing, *Advanced Powder Technology*, 28,2017,463.
- [2]. Saloni Sood, Arun Kumar, Neeraj Sharma, Photocatalytic and Antibacterial Activity Studies of ZnO Nanoparticles Synthesized by Thermal Decomposition of Mechanochemically Processed Oxalate Precursor, *Chemistry select*, 1, 2016, 6925.
- [3]. Thangavelu Kavitha, Anantha Iyengar Gopalan, Kwang-PillLee, Soo-YoungPark, Glucose sensing, photocatalytic and antibacterial properties of graphene-ZnO nanoparticle hybrids, *Carbon*, 50, 2012, 2994.
- [4]. N. Elavarasan, K. Kokila, G. Inbasekar, V. Sujatha, Evaluation of photocatalytic activity, antibacterial and cytotoxic effects of green synthesized ZnO nanoparticles by Sechium edule leaf extract, *Research on Chemical Intermediates*, 43, 2017, 3361.
- [5]. K. Pradeev Raj, K. Sadaiyandi, A. Kennedy, Suresh Sagadevan, Photocatalytic and antibacterial studies of indium-doped ZnO nanoparticles synthesized by co-precipitation technique, *Journal of Materials Science: Materials in Electronics*, 28, 2017, 19025.
- [6]. L.S Reddy Yadav, Danith kumar, C. Kavitha, H. Rajanaika, B. Daruka Prasad, Antibacterial and Photocatalytic activities of ZnO Nanoparticles : Synthesized using Water Milon Juice as Fuel, *International Journal on Nanoscience*, 15, 2016, 1.
- [7]. Lingling Wang, Long Shen, Luping Zhu, Haiying Jin, Naici Bing, and Lijun Wang, Preparation and Photocatalytic Properties of SnO_2 Coated on Nitrogen-Doped Carbon Nanotubes, *Journal of nanomaterials*, 2012,2012, 1.
- [8]. Amin ahmadpour, Mohsen Zare, Milad Behjoomanesh, Majid Avazpour, Photocatalytic decolorization of methyl orange dye using nano-photocatalyst, 1, 2015, 125.
- [9]. K.Akhil, J.Jayakumar, G.Gayathri, S. SudheerKhan, Effect of various capping agents on photocatalytic, antibacterial and antibiofilm activities of ZnO nanoparticles,160, 2016, 32.

- [10]. Si-Wei Zhao, Chong-Rui Guo, Ying-Zhu Hu, Yuan-Ru Guo, Qing-Jiang Pan, The preparation and antibacterial activity of cellulose/ZnO composite: a review, *Open chemistry*, 16, 2018, 9.
- [11]. K. Ravichandran, P. Philominathan, Investigations on microstructural and optical properties of CdS films fabricated by a low-cost, simplified spray technique using perfume atomizer for solar cell applications, *Solar Energy*, 82, 2008, 1062.
- [12]. A. Ayeshamariam, D. Saravanakumar, Kashif M, et al. Analysis on the effect of ZnO on Carbon nanotube by spray pyrolysis method, *Mechan Adv Mater Modern Process*, 2, 2016, 1.
- [13]. K.Kaviyarasu,A.Raja,P.A.DevarajanPA.etal.Structuralelucidationandspectralcharacterizations ofCo₃O₄nanoflakes.*Spectrochim Acta A*, 114, 2013, 586.
- [14]. D. Saravanakumar, S. Sivaranjani, K. Kaviyarasu, A. Ayeshamariam, B. Ravikumar, S. Pandiarajan, C. Veeralakshmi, M. Jayachandran, and M. Maaza, Synthesis and characterization of ZnO–CuO nanocomposites powder by modified perfume spray pyrolysis method and its antimicrobial investigation, 39, 2018, 032001.
- [15]. D. Saravanakumar, S. Sivaranjani, A. Ayeshamariam, B. Ravikumar, S. Pandiarajan, M. Jayachandran, Perfume Spray Analysis of Sn Doped ZnO-CNT NPs and its Morphological Characterizations, *Journal of Powder Metallurgy and Minings*, 6, 2017, 1000168.
- [16]. Viorica Musat, Mariana (Busila) Ibanescu, Dana Tutunaru, Florentina Potecasu, Fe-Doped ZnO nanoparticles:Structural, Morphological, Antimicrobial Photocatalytic Characterization, *Advanced Material Research*, 1143, 2017, 233.
- [17]. Mohammad Hossein, Ahmadi Azghandi, B.Vasheghani, F.F.H.Rajabi, M.Keramati, Synthesis of Cd doped ZnO/CNT nanocomposite by using microwave method: Photocatalytic behavior, adsorption and kinetic study, *Result in Physics*, 7, 2017, 1106.
- [18]. Hongxia Peng, Xiaohe Liu, Wei Tang, Renzhi Ma, Facile synthesis and characterization of ZnO nanoparticles grown on halloysite nanotubes for enhanced photocatalytic properties, *Scientific Report*, 7, 2017, 1.
- [19]. J.T. Seil, T.J. Webster, Antimicrobial applications of nanotechnology: Methods and literature. *Int. J. Nano. Med*, 7, 2012, 2767.
- [20]. R.Rusdi, A.A.Rahman, N.S.Mohamed, N.Kamarudin, N.Kamarulzaman, Preparation and band gap energies of ZnO nanotubes, nanorods and spherical nanostructures, *Powder Technol*, 210, 2011, 18.
- [21]. R. Andrews, D. Jacques, D. Qian, and T. Rantell, Multiwalled carbon nanotubes: synthesis and application, *Acc. Chem. Res*, 35, 2002, 1008.
- [22]. K. Kasinathan, J. Kennedy, E. Manikandan, Photodegradation of organic pollutants RhB dye using UV simulated sunlight on ceria based TiO₂ nanomaterials for antibacterial application, *Sci Rep*, 6, 2016, 38064.
- [23]. K. Bharathi Yazhini, H. Gurumalles Prabu, Antibacterial Activity of Cotton Coated with ZnO and ZnO-CNT Composites, *Applied Biochemistry and Biotechnology*, 175, 2015, 85.
- [24]. Li, H.; He, X.; Liu, Y.; Huang, H.; Lian, S.; Lee, S.-T.; Kang, Z. One-step ultrasonic synthesis of water-soluble carbon nanoparticles with excellent photoluminescent properties, *Carbon*, 49, 2011, 605.
- [25]. P. Wang, M. Cao, C. Wang, Y. Ao, J. Hou, J. Qian Kinetics and thermodynamics of adsorption of methylene blue by a magnetic graphene-carbon nanotube composite, *Applied Surface Science*, 290, 2014, 124.
- [26]. X. Wang, L. Zhi, K. Mullen, Transparent, conductive graphene electrodes for dye-sensitized solar cells, *Nano Lett*, 8, 2008, 323.
- [27]. G. Li, X. Zhu, X. Tang, W. Song, Z. Yang, J. Dai, Y. Sun, X. Pan, S. Dai Doping and annealing effects on ZnO: Cd thin films by sol-gel method, *Journal of Alloy Compound*, 509, 2011, 4816.
- [28]. Mohammad Hossein, Ahmadi Azghandi, B.VasheghaniF.H.Rajabi, M.Keramati, Synthesis of Cd doped ZnO/CNT nanocomposite by using microwave method: Photocatalytic behavior, adsorption and kinetic study, *Results in Physics*, 7, 2017, 1106.
- [29]. R. Saravanan, N. Karthikeyan, V. Gupta, E. Thirumal, P. Thangadurai, and V. Narayanan A. Stephen, ZnO/Ag nanocomposite: an efficient catalyst for degradation studies of textile effluents under visible light. *Mater Sci Eng. C*, 33, 2013, 2235.
- [30]. Minggui Wang, Yimin Hu, Jie Han, Rong Guo, Huixin Xiong and Yadong Yin, TiO₂/NiO hybrid shells: p–n junction photocatalysts with enhanced activity under visible light, *J. Mater. Chem A*, 3, 2015, 20727.
- [31]. U. Cihak, U, Characterization of residual stresses in turbine discs by neutron and high-energy X-ray diffraction and comparison to finite element modeling. *Mater.Sci. Eng. a-Struct.Mater. Prop.Microstruct.Process*, 1, 2006, 437.
- [32]. R. Andrews, D. Jacques, D. Qian, and T. Rantell, Multiwalled carbon nanotubes: synthesis and application, *Acc. Chem. Res*, 35, 2002, 1008.
- [33]. W. I. Milne, K. B. K. Teo, G. A. J. Amaratunga, P. Legagneux, L. Gangloff, J. P. Schnell, V. Semet, V. Thien Binh, O. Groening, Carbon nanotubes as field emission sources, *Journal of Materials Chemistry*, 14, 2004, 933.
- [34]. L.L. Beecroft, C.K. Ober, Nanocomposite Materials for Optical Applications, *Chemistry of Materials*, 9, 1997, 1302.
- [35]. P.K. Stoimenov, R.L. Klinger, G.L. Marchin, K.J. Klabunde, Metal oxide nanoparticles as bactericidal agents, *Langmuir*, 18, 2002, 6679.
- [36]. Shakeel Ahmed, Mudasar Ahmad, Babu Lal Swami, Saiqal kram, A review on plants extract mediated synthesis of silver nanoparticles for antimicrobial applications: A green expertise, *Journal of advanced Research*, 7, 2016, 17.
- [37]. T. Takeshima, L. Sun, Y. Wang, Y. Yamada, N. Nishi, T. Yonezawa, B. Fugetsu, Salmon milt, DNA as a template for the mass production of Ag nanoparticles, *Polym. J*, 2014, 46, 36.
- [38]. M.A.M. Khan, S. Kumar, M. Ahamed, S.A. Alrokayan, M. S. Alsalhi, M. Alhoshan, A.S. Aldwayyan, Structural and spectroscopic studies of thin film of silver nanoparticles, *Appl. Surf. Sci*, 24, 2011, 10607.
- [39]. Silvana Da Dalt, Annelise Kopp Alves, Carlos Pérez Bergmann, Preparation and Performance of TiO₂- ZnO/CNT Hetero-Nanostructures Applied to Photodegradation of Organic Dye, *Material Research*, 19, 2016, 1372.
- [40]. J. Wei, Y. Jia, Q. Shu, Z. Gu, K. Wang, D. Zhuang, G. Zhang, Z. Wang, J. Luo, A. Cao, D. Wu, Double-walled carbon nanotube solar cells. *Nano Lett*, 7, 2007, 2317.
- [41]. Savita Chaudhary, Yesbinder Kaur, Bhumika Jayee, Ganga Ram Chaudhary, Ahmad Umar, NiO nanodisks: Highly efficient visible-light driven photocatalyst, potential scaffold for seed germination of *Vigna Radiata* and antibacterial properties, *Journal of Cleaner Production*, 190, 2018, 563.
- [42]. A. Diallo, K. Kaviyarasua, S. Ndiaye, B. M. Mothudia, A. Ishaqa, V. Rajendran, M. Maaza, Structural, optical and photocatalytic applications of biosynthesized NiO nanocrystals, *Green Chemistry Letters and Review*, 11, 2018, 166.
- [43]. M. K. Shamsabadi, M. Behpour, A.K. Babaheidari, Z. Saberi, Efficiently enhancing photocatalytic activity of NiO-ZnO doped onto nanozeolite X by synergistic effects of p–n heterojunction, supporting and zeolite nanoparticles in photo-degradation of Eriochrome Black T and Methyl Orange. *J. Photochem. Photobiol. A*, 346, 2017, 133.
- [44]. N. Wang, C.Q. Liu, C. L. B. Wen, H. L. Wang, S. M. Liu, W. W. Jiang, W.P. Chai, Structural, electrical and optical properties of K-doped NiO films prepared by rapid pyrolysis 858 sol-gel technique, *Thin Solid Films*, 616, 2016, 587.
- [45]. L. Zhang, M. Qin, W. Yu, Q. Zhang, H. Xie, Z. Sun, Q. Shao, X. Guo, L. Hao, Y. Zheng, Heterostructured TiO₂/WO₃ Nanocomposites for Photocatalytic Degradation of Toluene under Visible Light. *J. Electrochemical Soc*, 164, 2017, 1086.

- [46]. Sherif Okeil, Jan Krausmann, Inga Donges, Sandra Pflieger, Jorg Engstler, Jorg J. Schneider, ZnS/ZnO@CNT and ZnS@CNT nanocomposites by gas phase conversion of ZnO@CNT: A systematic study of their photocatalytic properties, Dalton transaction, 46, 2017, 5189.

D. Saravanakkumar "Synthesis Of NiO Doped ZnO/MWCNT Nanocomposite And Its Charecterization For Photocatalytic & Anti Microbial Applications "IOSR Journal of Applied Physics (IOSR-JAP) , vol. 10, no. 3, 2018, pp. 73-83